Validation of non-classical homogeneous nucleation model for G-glass and L-glass formations in liquid elements with recent molecular dynamics simulations

Robert F. Tournier

Validation of Non-Classical Homogeneous Nucleation Model for G-Glass and L-Glass Formations in Liquid Elements with Recent Molecular Dynamics Simulations

Robert F. Tournier [1,2,3]

[1]*Univ. Grenoble Alpes, CNRS, Grenoble INP*, L.N.C.M.I., 38000 Grenoble, France,*

**Institute of Engineering Univ. Grenoble Alpes:*

[2]*Laboratoire des champs magnétiques intenses, 25 avenue des Martyrs,38042 Grenoble, France*

[3]*Institut Neel, CNRS, 25 avenue des martyrs, 38000 Grenoble. France*

robert.tournier@lncmi.cnrs.fr

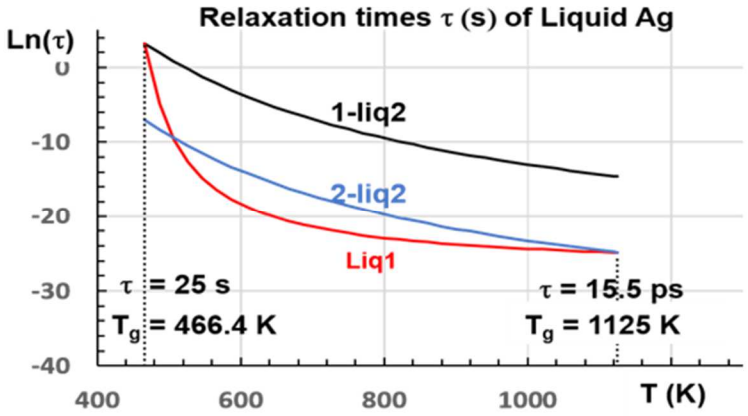

Liquid Ag with T_g = 466.4 K, heating rate of 1 K/s and T_g = 1125 K, heating rate of 1.6×10^{12} K/s predicted by the two associated models

Abstract: A first-order transition from liquid to homogenous glass denoted L-glass is predicted since 2016, in liquid elements having a Lindemann constant equal to 0.103, with a non-classical homogeneous nucleation model, accompanied by a latent heat of 10.5 % of the melting heat. The transition under pressure of ^{4}He is the first example of this phenomenon. Recent molecular dynamic simulations of Qi An et al identify, in addition, a first-order freezing transition from liquid (L) to metastable heterogenous solid-like phase, denoted as the G-glass, when a supercooled liquid evolves isothermally below its melting temperature T_m at deep undercooling. These observations are related to the general phenomenon of first-order transitions of glacial phases obtained by annealing above T_g at various heating or cooling rates or by isotherm annealing. The non-classical model of homogenous nucleation describes

the first-order transitions of L-glass and G-glass to liquid in perfect agreement with these simulations.

Keywords: Glasses, homogenous nucleation, molecular dynamics simulations, liquid elements, first-order transitions

Molecular dynamics simulations on systems ranging from 32,000 to 2,048,000 atoms identify "a first-order freezing transition from liquid (L) to metastable heterogenous solid-like phase, denoted as the G-glass, when a supercooled liquid evolves isothermally below its melting temperature T_m at deep undercooling. In contrast, a more homogenous liquid-like glass, denoted as the $_L$-glass, is achieved when the liquid is quenched continuously to room temperature with a fast-cooling rate of ~10^{11} K/s" [1,2].

The first-order configurational freezing of $_L$-glass in undercooled liquid elements having a Lindemann constant of 0.103 is predicted since 2016 with (1) at:

$$T_g = 0.3777 \times T_m, \quad (1)$$

accompanied by a latent heat equal to (2):

$$L = 0.10504 \times H_m, \quad (2)$$

using a non-classical homogeneous nucleation (NCHN) model where H_m is the melting enthalpy [3]. This model is built, year after year, starting in 1991 with texturing a high Tc superconductor by solidification in a high magnetic field [4] and showing that growth nuclei survive above the melting temperature in many materials up to a high temperature above which the liquid is homogenous [5-7]. The undercooling rate of liquid elements is reexamined in 2007 using Turnbull's and Vinet's works [8,9] and introducing a complementary enthalpy in the classical nucleation equation which leads to the presence of surviving crystals, melting at $T = 1.196 \times T_m$ instead of T_m. The transition of glass formers at T_g is viewed as due to a

homogenous nucleation temperature of a new liquid state below the thermodynamic transition at T_g [10,11]. The enthalpy coefficients of glasses in strong and fragile liquids and the rules of their formation are proposed for many molecular substances and metallic liquids [12].

These initial works are used to predict transitions accompanied by latent heats. The first example of a first-order transition at T_g is the transformation of liquid ^{4}He under pressure to $_L$-glass phase [13]. The latent heat of this transformation agrees with predictions [14]. A glacial phase results from liquid-liquid transition above T_g obtained in many molecular systems by isotherm annealing or spontaneous transformation below T_m during heating after a deep undercooling [15,16]. Then, all glacial phases are G-phases. The most known are triphenyl phosphite [17-19], d-mannitol [20], n-butanol [17,21-23], $Mg_{69}Zn_{27}Yb_4$ [24], water [25] and few polymers [26].

The NCHN model still predicts the formation temperature of these G-phases and their transition enthalpy [25,27]. For example, these quantities perfectly agree with the experimental thermodynamic properties characterizing the formation of G-phase in water and quasi-crystalline phase of $Mg_{69}Zn_{27}Yb_4$ only knowing T_g and T_m [24,28].

The purpose of this paper is to verify that the NCHN model predicts the formation conditions of glacial phases in Ag-Cu and Ag liquids at various heating rates as described by molecular dynamics (MD) simulations and to verify that the $_L$-glass properties at high heating rates are compatible with those predicted at low heating rates.

Liquid silver is expected to undergo a first-order transition to $_L$-glass at T_g = 466.4 K with a melting temperature T_m = 1234.9 K. The relaxation times τ given in seconds are calculated with a Vogel-Fulcher-Tammann (VFT) law for the liquid state 1, a VFT temperature $T_{0m} = T_m/3$ in (3) and an Arrhenius law for the liquid state 2 in (4) [3]:

$$\ln(\tau_1/s) = B_1/(T - T_m/3) + \ln(\tau_0), \quad (3)$$

$$\ln(\tau_2/s) = B_2/T + \ln(\tau_0), \quad (4)$$

the relaxation times τ_1 and τ_2 being respectively the steady-state nucleation time and the time-lag for the transient nucleation. These two relaxation times are assumed to be equal at the glass transition temperature.

For glass transition temperatures observed at high heating rates, the time τ'_0 in (5) is much weaker than τ_0:

$$\ln(\tau_2/s) = B_2/T + \ln(\tau'_0)\ . \quad (5)$$

The relaxation time equality $\tau_1 = \tau_2$ occurs at T_g = 466.4 K and 1125 K in Figure 1. The values of B_1, B_2 and T_m are 1669.1, 14209 K and 1234.9 K respectively for $\tau_1 = \tau_2$ = 25 s and then R = 1 K/s with a transition width $\Delta T = R\tau$ = 25 K. The glass transition at T_g = 1125 K is obtained with a heating rate R = 1.61×10^{12} K/s and the same ΔT. Other values of ΔT are possible varying τ_0.

The time τ_0 is equal to 1.5×10^{-12} s at T_g = 466.4 K and $\tau'_0 = 5.08\times10^{-17}$ s at 1125 K leading (5) to be equal to (4) at these temperatures. An average relaxation time of ≅110 ps at T = 800 K [2, Figure 3A] is used to determine $\tau_0 = 1.5\times10^{-12}$ s and the relaxation time is now given by (3) for each value of T_g.

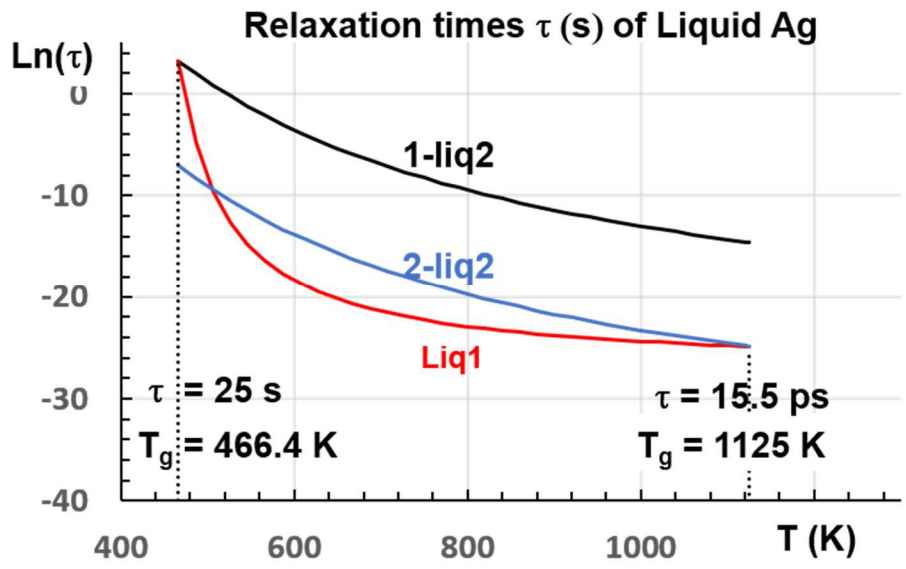

Figure 1: *The relaxation times of Ag liquids 1 and 2 with heating rate as hidden variable.* τ_1 *of Liq1 given by (3) with* $T_m/3 = 411.63$ *K;* τ_2 *of 1-liq2 and 2-liq2 given by (4),* $\tau_0 = 1.5\times10^{-12}$ s *and* 5.08×10^{-17} *s respectively. The two glass transition temperatures at 466.4 and 1125 K and relaxation times, 25 s and* 15.5×10^{-12} *s at these temperatures.*

The enthalpy coefficients of liquid states 1, 2 and 3 are given in (6-8):

Liquid 1

$$\varepsilon_{ls} = 0.217(1 - \theta^2/0.44444), \tag{6}$$

Liquid 2

$$\varepsilon_{gs} = 0.217(1 - \theta^2), \tag{7}$$

Phase 3

$$\Delta\varepsilon_{lg} = \varepsilon_{ls} - \varepsilon_{gs} = -0.27125 \times \theta^2. \tag{8}$$

The study of water and glacial phases has shown the presence in all glass-forming melts of a new phase called Phase 3 controlling the thermodynamic of all phase transformations with its enthalpy coefficient $\Delta\varepsilon_{lg}$ equal to the difference between those of liquids 1 and 2 [25,27]. A

first phase 3 is formed during the first heating from below the temperature T_3 where $\Delta\varepsilon_{lg} = -\Delta\varepsilon_{lg}(\theta = 0) = -\Delta\varepsilon_{lg0}$ [25]. This enthalpy coefficient difference $-\Delta\varepsilon_{lg0}$ belongs to the Gibbs free energy G_d of broken bonds in the configuron percolation model [29,30]. The system of bonds has two states, namely, the ground state corresponding to unbroken bonds and the excited state corresponding to broken bonds. It has been described by the statistics of two-level systems separated by the energy interval G_d. The Gibbs free energy of this Phase 3 is equal to G_d with the glass phase 3 entropy equal to zero up to T_g [28]. This is a homogeneous phase below T_g after cycling the sample temperature and heterogenous above T_g up to $T_{n+} > T_m$ involving an ordered liquid fraction of about 15% before melting at T_{n+}. This phase 3 is formed in liquid elements at $\theta_3 = -0.894$ ($T_3 = 130.9$ K in liquid Ag). Phase 3 is not surviving above T_m in liquid elements because $\Delta\varepsilon_{lg} = 0$ for $\theta = 0$ in (8) even if tiny crystals survive above T_m up to $\theta = \Delta\varepsilon_{lg}(\theta) = 0.19788$ (1479 K in liquid Ag) when (6) is applied [7,31]. These nuclei give rise to a critical temperature of superheating to obtain a maximum undercooling [32,33]. Phase 3 of configurons undergoes a second-order phase transition at T_g because the enthalpy coefficient $\Delta\varepsilon_{lg}$ is equal to zero at T_g in strong liquids or above T_g in fragile liquids. Pure liquid elements undergo a first-order transition at T_g because there is no temperature below T_m where $\Delta\varepsilon_{lg}$ is equal to zero. The configuron model also predicts that the first sharp diffraction minimum (FSDM) in the pair distribution function (PDF) contains information on structural changes in amorphous materials at the glass transition temperature T_g [30]. A sharp kink in FSDM occurs at the glass transition temperature T_g and this minimum of FSDM is obtained by MD simulations for Cu and Fe [34] and for nickel [30]. Phase 3 still appears as a generic name characterizing all hidden phases behind the glass phase such as stable and ultrastable phases obtained by vapor deposition and all phases induced above T_g by isothermal annealing or heating rate continuous increase such as ultrastable or glacial phases.

The glacial phase formation is governed by an enthalpy coefficient minimum $-\Delta\varepsilon$ of Phase 3 that is equal to -0.27125 for $\theta = -1$ or to -0.217 for $\theta = -0.89443$ in or to -0.12068 at $T = T_{0m}$

= 350 K for $\varepsilon_{ls} = 0$ [27]. The reduced homogeneous nucleation temperatures of L-glass ($\Delta\varepsilon$ = 0) and G-glass (Phase 3 with $\Delta\varepsilon$) are solutions of (9) for $\varepsilon_{gs0} = 0.217$:

$$\varepsilon_{gs0} = (3\theta_n + 2 - \Delta\varepsilon)/(1 - \theta_n^2). \quad (9)$$

Applying (9) to Liquid Ag, we deduce for $\Delta\varepsilon = 0.27125$, $\theta_n = -0.52375$, $T_n = 588.1$; for $\Delta\varepsilon = 0.217$, $\theta_n = -0.54336$, $T_n = 563.9$ K; for $\Delta\varepsilon = 0.12068$, $\theta_n = -0.5783$ and $T_n = 520.8$ K; for $\Delta\varepsilon = 0$, $\theta_n = -0.6223$ and $T_n = 466.4$ K.

ε_{gs0} depends on θ_g through (10)

$$\varepsilon_{gs0} = \left(3\theta_{gg} + 2\right)/(1 - \theta_{gg}^2). \quad (10)$$

Increasing the heating rate, increases θ_{gg}, ε_{gs0} and θ_n characterizing a G-phase. At each value of the glass transition θ_{gg} of the G-phase in (10), corresponds values of ε_{gs0} and θ_n given by (9) as shown in Figure 2 and:

(11) for $\Delta\varepsilon = 0.27125$

$$\theta_{gg} = 13.759\theta_n^3 + 25.779\theta_n^2 + 16.72\theta_n + 3.2034, \quad (11)$$

(12) for $\Delta\varepsilon = 0.217$

$$\theta_{gg} = 18.309\theta_n^3 + 31.108\theta_n^2 + 18.248\theta_n + 3.1451, \quad (12)$$

(13) for $\Delta\varepsilon = 0.12068$

$$\theta_{gg} = 36.474\theta_n^3 + 48.732\theta_n^2 + 22.276\theta_n + 2.928. \quad (13)$$

The lowest value of θ_{gg} in Figure 2 is –0.52375 for $\Delta\varepsilon = 0.27125$, –0.54336 for $\Delta\varepsilon = 0.217$ and –0.5783 for $\Delta\varepsilon = 0.12068$. They correspond to θ_n leading to the initial T_g at low heating rate.

The enthalpy coefficient $\Delta\varepsilon_{lgg}$ at θ_n is -0.27125 or -0.217 or -0.12068 for all liquids 2 for each value of ε_{gs0}. Applying (11) to liquid Ag with T_{gg} = 1125 K = $(1+\theta_{gg}) \times T_m$, we obtain θ_n = -0.35245 and T_n = 799.7 K in good agreement with [2].

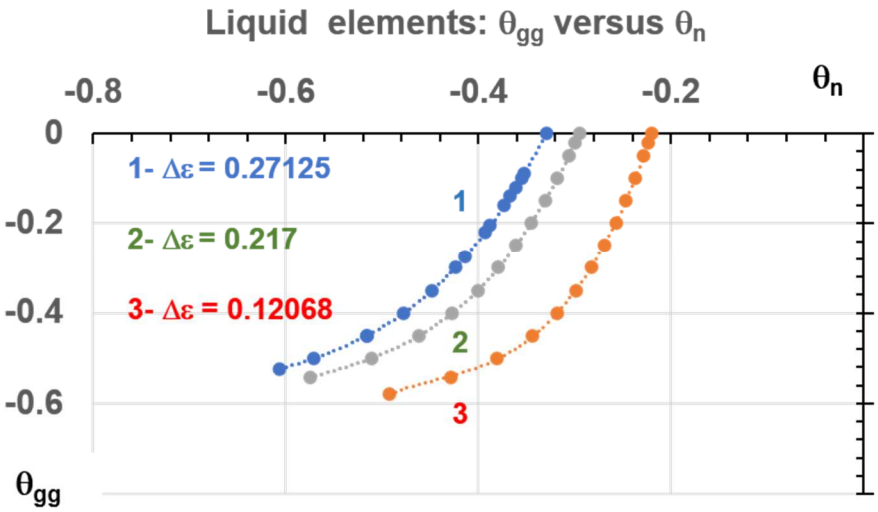

Figure 2*: The reduced glass transition temperatures θ_{gg} of G-phase and Phase 3 versus the reduced homogeneous nucleation temperature θ_n in liquid elements for $\Delta\varepsilon$ = 0.27125, 0.217, and 0.12068.*

The molecular dynamics simulations show that G-phase coexists with liquid phase above T_n [(1) (2)]. The G-phase enthalpy coefficient $\Delta\varepsilon_{lgg}$ at T_{gg} characterizes a first-order transition at T_{gg} and is equal, for Liquid Ag, to $0.10504 \times T_{gg}/466.4+(0.27125-0.10504) \times T_{gg}/588.1$ leading to (14) in liquid Ag because the L-glass and G-glass are melted at the same temperature T_{gg}:

$$\Delta\varepsilon_{lgg} = 5.08 \times 10^{-4}\, T_{gg}, \qquad (14)$$

Applying (14) with T_{gg} = 1125 K leads to $\Delta\varepsilon_{lgg}$ = 0.571 in perfect agreement with the MD simulations for liquid Ag [1, Figure 4a] showing that $\Delta\varepsilon_{lgg}$ = 71 mev/124.9 mev = 0.568. (The melting enthalpy is chosen by [2] as equal to 124.9 mev/atom). The temperature T_{gg} cannot be higher than the crystallization temperature T_x. Assuming that T_x cannot be higher

than T_m, the maximum of T_{gg} is T_m defined by θ_n = -0.32939 in (11) and the maximum of $\Delta\varepsilon_{lgg}$is 0.627 in liquid Ag.

The Lindemann constant is assumed to be 0.103 in this alloy. Applying (1) to $Cu_{75}Ag_{25}$ liquid leads to T_g = 450.6 K with T_m = 1193.1 K [35]. The melting temperature T_m = 1050 K (and T_g = 396.6 K with (1)) agrees with the simulation choice and permits the comparison of the two models. Consequently, T_m = 1050 K and T_g = 396.6 K fix the relaxation times of $_L$-glass in (15-18):

Liq1 (for all values of T_g)

$$\ln(\tau_1/s) = 1592.2/(T - 350) - 28.186, \quad (15)$$

1-Liq2 (T_g = 396.6 K)

$$\ln(\tau_2/s) = 13556.3/T - \ln(5.74 \times 10^{-13}). \quad (16)$$

The value $\tau_0 = 5.74 \times 10^{-13}$ ($\ln \tau_0 = -0.28186$) comes from the "measurements" of the transition width $\Delta T \cong 150.6$ K from T_g = 716.4 K corresponding to T_n = 716.4 K for T_{gg} = 945 K and a relaxation time of 44.3 ps with a heating rate R = 3.4×10^{12} K/s as shown in Figure 4 for $_L$-glass [1]. The relaxation time at T_g = 396.6 K is 402 s with ΔT = 150.6 K and R = 0.374 K/s (22.4 K/min).

The relaxation time τ_2 is given by (15) for each value of T_g. Ln (τ'_0) in (17,18) is defined for each value of T_g even for $T_g = T_m$ = 1050 K.

2-Liq2 (T_g = 1050 K)

$$\ln(\tau_2/s) = 13556.3/T - 38.822\ , \quad (17)$$

3-Liq2 (T_g = 716.4 K)

$$\ln(\tau_2/s) = 13556.3/T - 42.763. \quad (18)$$

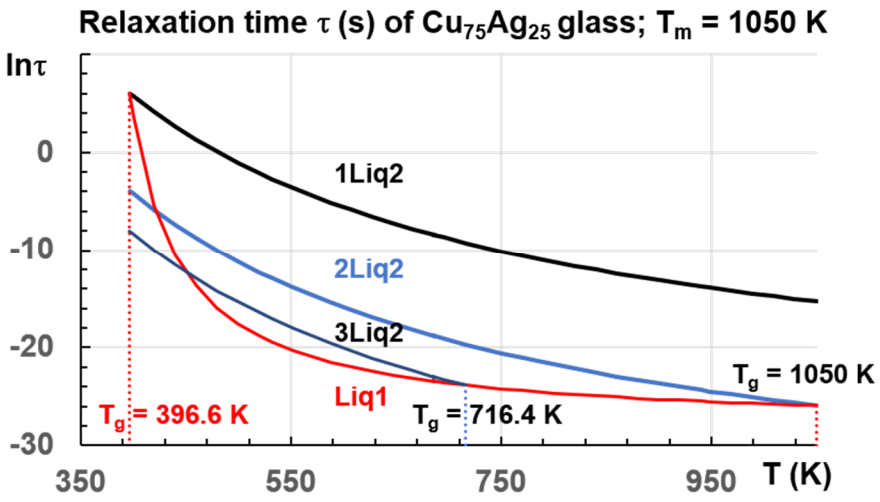

Figure 3: *$Cu_{75}Ag_{25}$ relaxation times $\tau(s)$ versus T (K) with heating rate as hidden variable. Liq1 with (15), 1Liq2 with (16), 2Liq2 with (17), 3liq2 with (18). T_g = 396.6 K, τ = 402 s, ΔT = 150.6 K, heating rate R = 0.374 K/s; T_g = 716.4 K, ΔT = 150.6 K, τ = 44.3 ps, R = 3.4×10^{12} K/s; T_g = 1050 K, ΔT = 150.6 K, τ = 5.58 ps, R = 2.68×10^{13} K/s.*

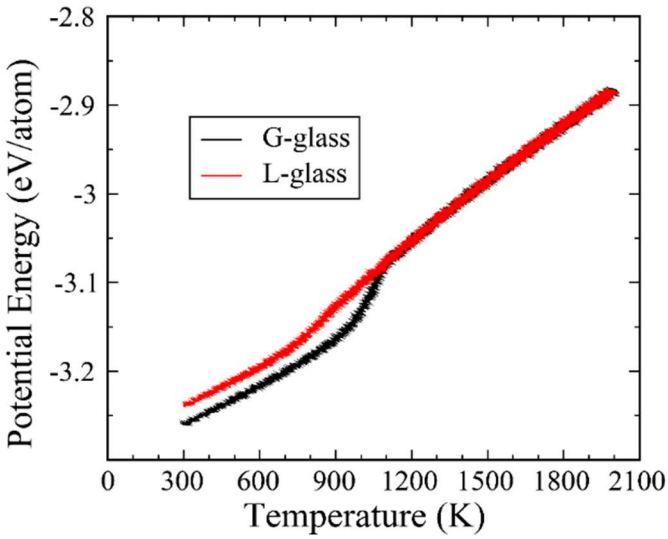

Figure 4: *Remelting of G-glass and L-glass phases with a heating rate of 3.4×10^{12} K/s. reproduced from [1 Figure S4] with ACS permission: Q. An, W.L. Johnson, K. Samwer, S.L. Corona, and W. A. Goddard III. J. Phys. Chem. Lett. 11 (2020) 632-645. The G-glass potential energy change at T_g is much higher than that of $_L$-glass.*

The enthalpy coefficient minimum $\Delta\varepsilon$ can be equal to 0.217 or 0.12068 at the nucleation temperature T_n of G-glass because $\Delta\varepsilon_{lgg}$ is much weaker in liquid Ag-Cu than in pure liquid Ag [1, Figure 4a]. The initial homogeneous nucleation temperature of G-phase is T_n = 544.82 K for $\Delta\varepsilon$ = 0.217 applying (9).

The enthalpy coefficient change increases with the heating rate and is equal to $0.10504\times T_{gg}/396.6+(0.217-0.10504)\times T_{gg}/544.82 = 4.703\times T_{gg}$ for $\Delta\varepsilon$ = 0.217 where T_{gg} is the glass transition temperature above the nucleation temperature T_n of G-glass as defined by (12). For T_{gg} = 945 K, the enthalpy coefficient is $\Delta\varepsilon_{lgg}$ = 0.444. This value is in good agreement with the potential energy changes in Figure 4 and the jump of $_L$-glass is about 2 times weaker than that of G-glass at the glass transition.

Figure 5 shows that the change of potential energy at 700 K is about 24 mev/atom. This value is compatible with $\Delta\varepsilon$ = 0.12068 because $\Delta\varepsilon_{lgg} = 0.10504\times T_{gg}/396.6+(0.12068-0.10504)\times T_{gg}/544.82 = 2.935\times T_{gg} = 0.2055$ for T_{gg} = 700 K. The melting heat at 1050 K deduced from the Cu melting entropy is evaluated to ~105 mev/atom. Then, $\Delta\varepsilon_{lgg}\times 105$ ~21.7 mev agrees with [1, Figure 4a].

The G-phase enthalpy coefficient change $\Delta\varepsilon$ increases with heating rate following the singular values of Phase 3 which are equilibrium values and leads, step-by-step, to successive first-order transitions [27]. These effects are confirmed by more examples of enthalpy jumps at low heating rates in a metallic liquid [36] and multiple cooling rates generating different types of monolithic metallic glasses [37].

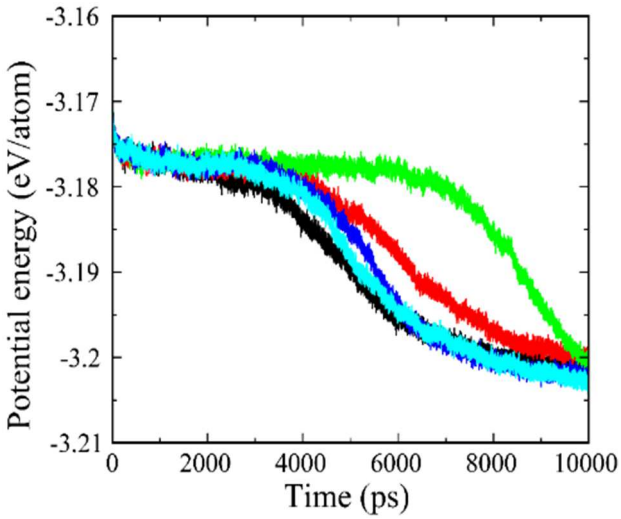

Figure 5: *5 isothermal runs for a system of 32000 atoms at 700 K for $Cu_{75}Ag_{25}$ reproduced from [1, Figure S1] with ACS permission: Q. An, W.L. Johnson, K. Samwer, S.L. Corona, and W. A. Goddard III. J. Phys. Chem. Lett. 11 (2020) 632-645.*

Pure copper is characterized by T_m = 1358 K, T_g = 512.16 K applying (1) and T_n = 646.7 applying (9). The new enthalpy coefficient $\Delta\varepsilon_{lgg}$is given in (16):

$$\Delta\varepsilon_{lgg} = 4.62 \times 10^{-4}\, T_{gg}. \qquad (16)$$

The enthalpy coefficient change maximum at $T_{gg} = T_m$ is still equal to 0.627. Nevertheless, $\Delta\varepsilon_{lgg}$is weaker in liquid copper for the same T_{gg} as compared to liquid Ag and as observed in MD simulations.

The G-glass phases represented in Figures 4 and 5 are characterized by T_{gg} = 945 and 700 K and T_n = 716.4 and 637.5 K as indicated in Table 1. The isothermal relaxation times τ_g = $\Delta T/R$ at T_{gg} are deduced from the transition width ΔT (K) and the applied heating rate R (K/s). The transition width ΔT = 150 K is broad as observed in Figure 4. The initial glass transition at T_g = 350 K in Figure 3 has the same width.

The NCHN model predicts all observed relaxation times of G-glass from 44.3 ps at T_{gg} = 945 K to 4430 ps at 700 K as shown in Figures 4 and 5. A relaxation time of 402 s and a heating

rate of 22 K/min are obtained at T_g = 396.6 K. A prediction of a heating rate leading to T_{gg} = T_m = 1050 K is proposed. The time τ_0 is a little weaker for the G-glass than for the L-glass.

Table 1. ***$Cu_{75}Ag_{25}$.*** *T_g (K) the glass transition temperature of L-phase; T_{gg} (K) the glass transition temperature of the G-phase; T_n (K) = T_g (K) the homogenous nucleation temperature of the G-phase equal to the glass transition temperature T_g (K) of the corresponding L-phase; ΔT the width of the glass transition; B_1 (K) defined by (3); B_2 (K) defined by (4); R (K/s) the cooling rate; ln(τ_g) the neperian logarithm of the relaxation times $\tau_g = \tau_1 = \tau_2$ at the glass transition; τ_0 (s) defined by (5).*

	T_g(K)	T_{gg}(K)	T_n (K)	ΔT (K)	B_1 (K)	B_2 (K)	R (K/s)	lnτ_g	τ_g (s)	τ_0 (s)
G-glass		1050	740.65	150	5877	8815	3.4×10^{12}	-23.84	44.3×10^{-12}	1×10^{-14}
G-glass		945	716.4	150	4995	7934	3.4×10^{12}	-23.84	44.3×10^{-12}	1×10^{-14}
G-glass		700	637.5	150	4552	9104	3.4×10^{10}	-19.23	4430×10^{-12}	1×10^{-14}
L-glass	1050			150	1592.3	13556	2.7×10^{13}	-25.91	5.58×10^{-12}	5.74×10^{-13}
L-glass	740.6			150	1592.3	13556	3.4×10^{12}	-24.11	33.8×10^{-12}	5.74×10^{-13}
L-glass	716.4			150	1592.3	13556	3.4×10^{12}	-23.84	44.3×10^{-12}	5.74×10^{-13}
L-glass	637.5			150	1592.3	13556	3.4×10^{10}	-22.65	4430×10^{-12}	5.74×10^{-13}
L-glass	396.6			150	1592.3	13556	0.374	6	402	5.74×10^{-13}

In conclusion, recent MD simulations prove that the various glass formations, resulting from first-order transitions at high heating and cooling rates in liquid elements, are governed by the enthalpy differences $\Delta\varepsilon_{lg}(\theta) = \varepsilon_{lg}(\theta) - \varepsilon_{gs}(\theta)$ of liquids 1 and 2 and formed at the nucleation temperatures $\theta_n = (T_n - T_m)/T_m$ predicted by the NCHN model. Successive first-order transitions to various glacial phases governed by singular values of $\Delta\varepsilon_{lg}$ are expected depending on the heating rate. Values such as -0.27125, 0.217, 0.12068 are observed and could lead to new glass equilibrium enthalpies by cooling below T_n. The G-glass phase tends

to relax toward the liquid state between T_n and T_{gg} as observed in several glacial phases in agreement with the metastable heterogenous solid-like phase observed by MD simulations. The agreement is quantitative for liquid elements having a Lindemann constant equal to 0.103 corresponding to $\varepsilon_{lg}(\theta = 0) = \varepsilon_{gs}(\theta = 0) = 0.217$ at T_m. The enthalpy coefficient maximum inducing the last first-order transition before crystallization is 0.27125 as expected from the NCHN model applied to liquid Ag.

Acknowledgments: Thanks to Grenoble Alpes University and Laboratoire national des champs intenses de Grenoble.

Declaration of competing Interests

The author declares no competing interest.

References

1. Q. An, W.L. Johnson, K. Samwer, S.L. Corona, W.A. Goddart III, Acta Mater. 195 (2020) 274-281.

2. Q. An, W.L. Johnson, K. Samwer, S.L. Corona, and W. A. Goddard III, J. Phys. Chem. Lett.11 (2020) 632-645.

3. R.F.Tournier, Chem. Phys. Lett. 651 (2016). Corrig: Chem. Phys. Lett. 675 (2017) 174.

4. P. de Rango, M. Lees, P. Lejay, A. Sulpice, R. Tournier and M. Ingold, P. Germi, & M. Pernet, Nature. 349 (1991) 770-772.

5. R.F. Tournier and E. Beaugnon, Sci. Technol. Adv. Mater. 10 (2009) 014501.

6. L. Porcar, P. de Rango, D. Bourgault, and R. Tournier, Magnetic texturing of high-Tc superconductors, in Alexander Gabovitch [ed.]. Superconductors: materials, properties and applications. s.l. : Intech, 2012, 8. http://dx.doi.org/10.5772/48698.

7. R.F. Tournier, Metals, 4 (2014) 359-387.

8. D. Turnbull, J. Chem. Phys. 20 (1952) 411.

9. P. Vinet, L. Magnusson, H. Frederikssen, P.J. Desré, J. Colloid Interf. Sci. 255 (2002) 363-374.

10. R.F. Tournier, Sci. Technol. Adv. Mater. 10 (2009) 014617.

11. R.F Tournier, Materials, 4 (2011) 869-892.

12. R.F. Tournier, Physica B, 454 (2014) 253-271.

13. J. Bossy, T. Hansen, and H.R. Glyde, Phys. Rev. B, 81 (2010) 184507.

14. R.F. Tournier, J. Bossy, Chem. Phys. Lett. 658 (2016) 282-286.

15. A. Ha, I. Cohen, X. Zhao, M. Lee, and D. Kivelson, J. Phys. Chem. Lett. 100 (1996) 1-4.

16. D. Kivelson, S.A. Kivelson, X. Zhao, Z. Nussinov, G. Tarjus, Physica A, 219 (1995) 27-38.

17. M. Kobayashi, and H. Tanaka, Nature Comm. 7(2016) 13438.

18. K.V. Miltenburg and K. Blok, J. Phys. Chem. 100 (1996) 16457-16459.

19. H. Tanaka, J. Non-Cryst. Sol. 351 (2005) 3371-3384.

20. M. Zhu, J-Q Wang, J.H. Perepezko, and L. Yu, J. Chem. Phys. 142 (2015) 244504.

21. A.I. Krivchikov, M. Hassaine, I.V. Sharapova, O.A. Korolyuk, R.J. Jimenez-Rioboo, M.A. Ramos, J. Non-Cryst. Sol. 357 (2011) 524-529.

22. B.V. Bolshakov, A.G. Dzhonson, J. Non-Cryst. Sol. 351 (2005) 444-454.

23. R. Kurita, and H. Tanaka, J. Phys.: Condens. Matter. 17 (2005) L293-L302.

24. G. Kurtuldu, K.F. Shamlaye, and J. Loffler, PNAS. 115 (24) (2018) 6123-6128.

25. R.F. Tournier. Physica B, 579 (2020) 411895.

26. R. F. Tournier, and M. I. Ojovan, Physica B, 2021.

27. R.F. Tournier. Chem. Phys. 524 (2019) 40-54.

28. R.F. Tournier and M. Ojovan, Physica B, 602 (2021) 412542.

29. M.I. Ojovan, J. Non-Cryst. Sol. 382 (2013) 79.

30. M.I. Ojovan, D.V. Louzguine Luzgin, Physica B,124 (2020) 3186-3194.

31. R. F. Tournier, Physica B, 392 (2007) 79-91.

32. B. Yang, J.H. Perepezko, J.W.P. Schmelzer, Y. GaO, and C. Schick, J. Chem. Phys. 140 (2014) 104513.

33. Y. He, J. Li. J. Wang, H. Kou, E. Beaugnon, Applied Physics A, 123 (2017) 391.

34. A.I. Bazlov, D.V. Louzguine-Luzguin, Metals, 10 (2020) 1532.

35. P.R. Subramanian, and J.H. Perepezko. J. Phase Equilibria. 14 (1993) 62-75.

36. J. Shen, Z. Lu, J. Q. Wang, S. Lan, F. Zhang, M. W.Chen, X. L. Wang, P. Wen, Y. H. Sun, H. Y. Bai, and W. H. Wang, J. Phys. Chem Lett. 11 (2020) 6718-6723.

37. J. E. K. Schawe, and J. F. Löffler, Nature Comm. 10 (1) (2019) 1337.